European Journal of Human Genetics (2014) 22, 1314–1320

www.nature.com/ejhg

ARTICLE

Cell therapy using retinal progenitor cells shows therapeutic effect in a chemically-induced rotenone mouse model of Leber hereditary optic neuropathy

Fiona C Mansergh*[,1], Naomi Chadderton[1], Paul F Kenna[1,2], Oliviero L Gobbo[3] and G Jane Farrar[1]

Primary mitochondrial disorders occur at a prevalence of one in 10 000; ~50% of these demonstrate ocular pathology. Leber hereditary optic neuropathy (LHON) is the most common primary mitochondrial disorder. LHON results from retinal ganglion cell pathology, which leads to optic nerve degeneration and blindness. Over 95% of cases result from one of the three common mutations in mitochondrial genes MTND1, MTND4 and MTND6, which encode elements of the complex I respiratory chain. Various therapies for LHON are in development, for example, intravitreal injection of adeno-associated virus carrying either the yeast NDI1 gene or a specific subunit of mammalian Complex I have shown visual improvement in animal models. Given the course of LHON, it is likely that in many cases prompt administration may be necessary before widespread cell death. An alternative approach for therapy may be the use of stem cells to protect visual function; this has been evaluated by us in a rotenone-induced model of LHON. Freshly dissected embryonic retinal cells do not integrate into the ganglion cell layer (GCL), unlike similarly obtained photoreceptor precursors. However, cultured retinal progenitor cells can integrate in close proximity to the GCL, and act to preserve retinal function as assessed by manganese-enhanced magnetic resonance imaging, optokinetic responses and ganglion cell counts. Cell therapies for LHON therefore represent a promising therapeutic approach, and may be of particular utility in treating more advanced disease.
European Journal of Human Genetics (2014) **22,** 1314–1320; doi:10.1038/ejhg.2014.26; published online 26 February 2014

INTRODUCTION

Primary mitochondrial disorders (those caused by mutations in the mitochondrial genome) occur at a prevalence of ~1 in 10 000, with 1 in 200 individuals carrying at-risk mutations.[1] Approximately 50% demonstrate some form of ocular pathology.[2] Mitochondria provide energy in the form of ATP generated by oxidative phosphorylation; therefore, mitochondrial mutations primarily affect tissues with the greatest energy requirements, such as the retina, the inner ear, central and peripheral nervous systems and cardiac and skeletal muscle.[2,3]

Leber hereditary optic neuropathy (LHON) is the most common primary mitochondrial disorder, with a prevalence of ~1 in 31 000–50 000 in northern Europe. The prevalence of at-risk carriers is much higher, estimated at 1 in 8 500 in the UK; furthermore, primary LHON mutations were found in 1 out of 350 neonatal umbilical cord samples.[1,4] LHON is maternally inherited, often results from homoplasmy of the causative mitochondrial mutation, and is incompletely penetrant; visual loss occurs in 50% of males and 10% of females. Symptoms result from retinal ganglion cell (RGC) pathology, which leads to RGC death via apoptosis, resulting in optic nerve degeneration and subsequent blindness. Nonocular symptoms of mitochondrial dysfunction may also be present.[1,4]

Although many mutations implicated in LHON have been described, 90–95% of the cases result from one of the three common mutations in mitochondrial genes including MTND1, MTND4 and MTND6, which encode elements of the complex I respiratory chain (MTND1*LHON3460A, OMIM 516000.0001, MTND4*LHON 11778A, OMIM 516003.0001, MTND6*LHON14484C, OMIM 516006.0001). The mitochondrial respiratory NADH-ubiquinone oxidoreductase complex, (Complex I), is composed of 44–45 subunits, seven of which are mitochondrially encoded, and is involved in transfer of electrons from NADH to ubiquinone (coenzyme Q).[2] Complex I deficit results in reduced oxygen consumption, increased reactive oxygen species, decreased energy supply and sensitization of the mitochondrial permeability transition pore (mtPTP) to apoptosis.[3,5] The retina is uniquely vulnerable to such insults, given its high energy demands and the nonreplicating nature of mammalian retinal neurons.[2,3,5]

LHON is similar in etiology to dominant optic atrophy (DOA), which has been mapped to seven loci, with three genes (OPA1, OPA3 and TMEM126A/OPA7) identified to date. These DOA genes are nuclear encoded, but have mitochondrial functions.[4,6] RGC dysfunction, accompanied by a much slower degeneration, also underlies primary open angle glaucoma (POAG). Notably, polymorphisms in the OPA1 gene have been associated with normal tension glaucoma,[7] and POAG lymphoblasts show complex I dysfunction.[8] Therapeutic development for LHON has been impeded by the need to target therapeutic agents to mitochondria, and the difficulty of engineering animal models carrying specific mtDNA mutations, although recently a mouse model carrying a mtDNA mutation has been shown to demonstrate LHON-like

[1]Ocular Genetics Unit, Smurfit Institute of Genetics, School of Genetics and Microbiology, Trinity College Dublin, Dublin, Ireland; [2]Research Foundation, The Royal Victoria Eye and Ear Hospital, Dublin, Ireland; [3]School of Pharmacy and Pharmaceutical Sciences and Trinity College Institute of Neuroscience, Trinity College Dublin, Dublin, Ireland
*Correspondence: Dr FC Mansergh, Smurfit Institute of Genetics, University of Dublin, Trinity College, Lincoln Place Gate, Dublin 2, Ireland. Tel: +353 1 896 2484; Fax: +353 1 896 3848; E-mail: mansergf@tcd.ie
Received 20 September 2013; revised 19 December 2013; accepted 26 December 2013; published online 26 February 2014

symptoms.[5] We have utilized a chemically-induced model, the complex I inhibitor rotenone, to model LHON in mice. Rotenone inhibits the reduction of ubiquinone and causes specific and irreversible retinal effects in mice, which mimic those of LHON, when administered intravitreally.[3,9–11]

Intravitreal injection of an adeno-associated virus carrying the yeast NDI1 gene (AAV-NDI1) into rotenone-treated animals results in visual improvement as assessed by manganese-enhanced magnetic resonance imaging (MEMRI), RGC cell counts and optokinetic responses.[3] Given the rapid course of the disease in some LHON patients, prompt administration of the gene therapy may be necessary to provide benefit after diagnosis. As an alternative, we have examined the use of stem cells to protect visual function in a rotenone model of LHON. A small proportion of LHON patients show spontaneous reversal of symptoms, suggesting that even later stages of disease may possibly be amenable to therapeutic intervention. We have found that freshly dissected embryonic retinal cells do not integrate into the ganglion cell layer (GCL), unlike similarly obtained photoreceptor precursors, which can integrate retinally and act to preserve vision in models of RP.[12,13] However, in the current study we have established that the cultured retinal progenitor cells (RPCs) can integrate alongside the GCL, and preserve retinal function as assessed by MEMRI, optokinetic responses and RGC counts. Cell therapies for LHON therefore represent a promising therapeutic approach and may be of particular utility in treating advanced disease.

MATERIALS AND METHODS

Animal husbandry

Wild type 129Sv/J mice and enhanced green fluorescent protein (eGFP) mice were maintained under specific pathogen-free housing conditions. All procedures were carried out in adherence with EU law and Irish Department of Health and Children/Irish Medicine Board licence and permits. All procedures are compliant with the Association for Research in Vision and Ophthalmology statement for animal use. Where embryo-derived retinal samples were required, timed matings were carried out, followed by embryo dissection at E16 and E17. Adult mice were killed via CO_2 asphyxia or cervical dislocation, while embryos and pups were killed via decapitation.

Cell isolation

Pregnant animals were killed at 16 and 17 days *post-coitum*. The uterus was dissected free of other abdominal organs and placed in phosphate buffered saline (PBS). Embryos were dissected free of extraembryonic membranes and placed under UV light to identify eGFP-positive embryos, which were then decapitated. Retinas were dissected as described previously.[14] Cells were resuspended in volumes such that 3 μl contained 200 000 cells. For postnatally-derived retinal cells, eGFP-positive pups were identified via UV light exposure and decapitated before retinal dissection, otherwise the procedure was identical to that described above. Cells were then either intravitreally injected or placed in tissue culture for expansion as RGCs. Mouse embryonic fibroblasts (MEFs) were isolated as previously described.[15]

Intravitreal injections

Adult mice were anaesthetized and intravitreally injected with 0.6 μl, 1.5 or 2.5 mM rotenone or 0.6 μl dimethyl sulphoxide (DMSO) as described previously.[3] A week later, the same mice were similarly intravitreally injected with 3 μl RPCs or Hanks-balanced salt solution (HBSS). The second injection of cells or HBSS was used to assess lens health, as rotenone can cause cataracts. Animals with significant lens opacities at this stage were excluded from further analysis; large cataracts impair vision regardless of control or experimental status, thereby affecting the accuracy of optokinetic results in particular.

Cell culture

Following dissociation, 1×10^6 retinal cells were plated in T25 flasks (Sarstedt, Drinagh, Co., Wexford, Ireland) in optimized RPC medium as described previously.[14] Cells were differentiated via withdrawal of epidermal growth factor for 5 days, then harvested for injection. Cultured eGFP RPCs were harvested for injection as described previously,[14] resuspended in HBSS such that 3 μl contained 200 000 cells, and placed on ice until injection. MEFs were isolated and cultured as described previously.[15] MEFs were resuspended such that 3 μl contained 100 000 cells. This represented a maximum density as the MEFs were much larger and more viscous than RPCs and tended to block the syringe.

Histology and cell counts

Fixation, cryosectioning and staining were carried out as previously described.[16] 10 μm sections were obtained using a CM1900 cryostat (Leica, Wetzlar, Germany) and placed on poly-L-lysine coated microscope slides. For eGFP-labeled cell counts alone, all sections from a given eye were stained with 1 ng/ml DAPI, (Sigma-Aldrich, Arklow, Ireland) and mounted using AquaPolyMount (Polysciences, Eppelheim, Germany). Transplanted eGFP-positive cells retained after a month were then counted using a Zeiss Axioplan 2 fluorescent microscope (Carl Zeiss Ltd., Welwyn Garden City, UK). Signals obtained following photography with different filters were overlaid using Adobe Photoshop, CS6E (Adobe Systems Europe, Glasgow, UK). NeuN (also known as Fox3) staining and ganglion cell counts were obtained as described previously using 1/100 dilution of Fox3 antibody (Abcam, Cambridge, UK).[3] Eight to ten central retinal counts were obtained per eye; number of eyes analysed per group (n) is indicated in Figure 1. Counts for eGFP-positive cells were obtained from four separate series of injections (four separate cell preparations), and NeuN counts were obtained from a different four separate sets of injections (also four cell preparations). GFAP staining was carried out similarly to NeuN, with a 1/500 dilution of antiGFAP primary antibody (Sigma-Aldrich).

Manganese-enhanced magnetic resonance imaging (MEMRI)

MEMRI identifies active regions of the brain via the ability of manganese ions (Mn^{2+}) to enter excitable cells through voltage-gated calcium channels, thereby giving a good measure of the integrity of the optic nerve via its relative ability to transport Mn^{2+}.[17] Mice were anaesthetized and intravitreally injected with 2 μl of 20 mg/ml manganese chloride in PBS. Optic nerve integrity was then assessed using a 7-T Bruker Biospec 70/30 magnet (Bruker Biospin, Etlingen, Germany) as previously described.[3] Image J (NIH, Bethesda, MD, USA; http://imagej.nih.gov/ij) was used with MR images to quantify the region immediately superior to the optic chiasm. The intensity of the signal in the region of interest was divided by the intensity of the reference signal of an invariant anatomic area (the olfactory bulb). This measurement provided a normalized signal for each MRI scan. Data were obtained from four separate series of injections (four separate cell preparations).

Optokinetics

Optokinetic analysis measured murine response to moving stripes in a chamber created via four computer monitors, which projected images visible from a mouse-supporting platform in the centre of the square. A video camera placed above the chamber allowed the observer to view slow tracking movements made by the mouse in response to the moving images. The direction of apparent rotation was reversed intermittently in order to assess visual response from each eye. The thickness of the stripes was reduced in a stepwise manner until the mouse could no longer register the movement and therefore stopped tracking. This optokinetic response spatial-frequency threshold was measured blind for experimental and control mice using the OptoMotry optokinetics system (VOS,Cerebral Mechanics, Lethbridge, Canada) as described previously.[3] Data were obtained from five separate series of injections (five separate cell preparations).

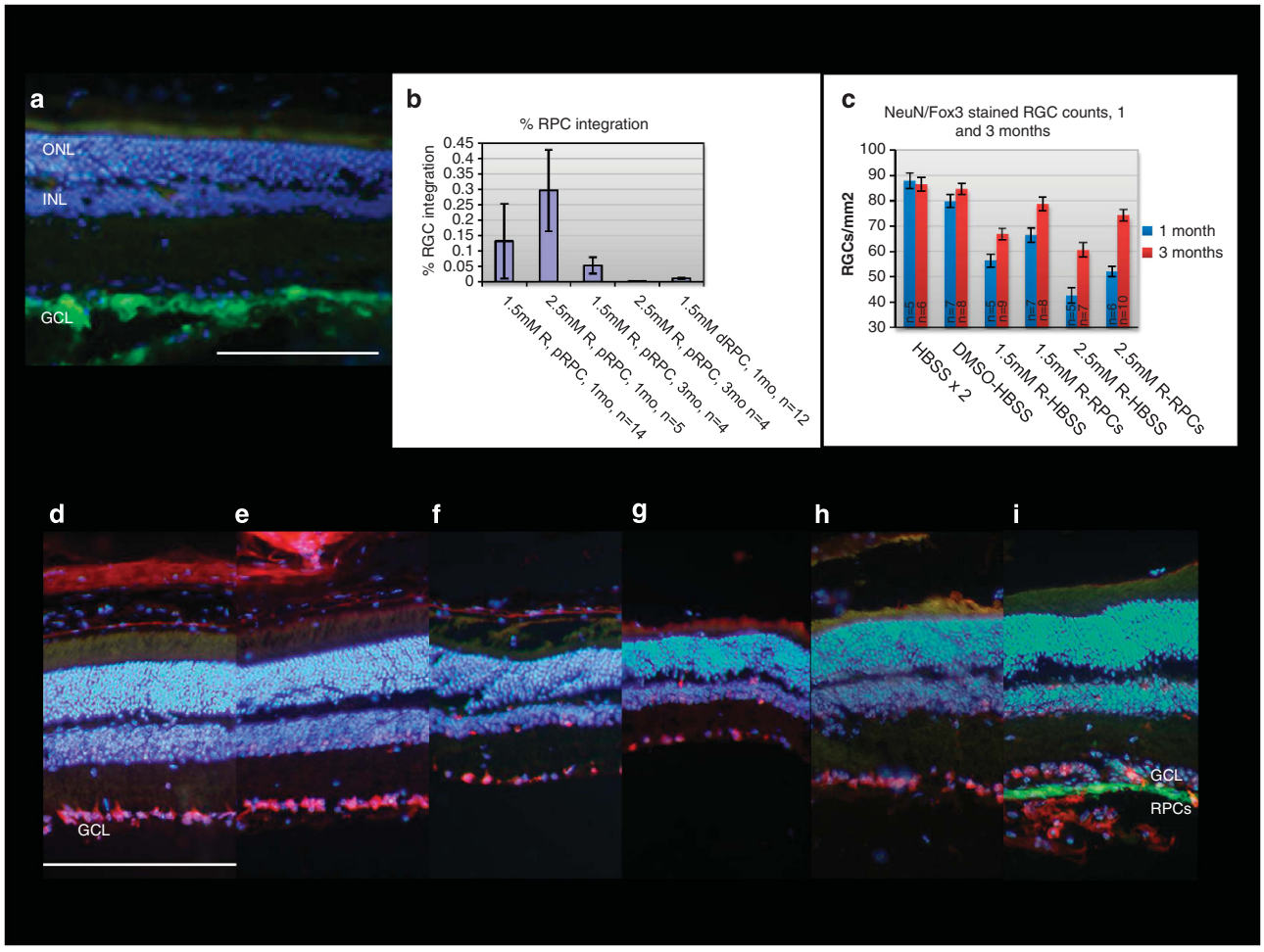

Figure 1 Cell and RGC counts. (**a**) Transplanted pRPCs (eGFP positive). (**b**) RPC counts in rotenone + RPC-transplanted retinas, expressed as a percentage of transplanted cells (200 000 RPCs). (**c**) RGC counts, from Fox3/NeuN-stained retinas at 1 month and 3 months, from control, rotenone-treated and rotenone + RPC-treated animals, $n = 5$–10 eyes/category, see graph for details. R, Rotenone. *P*-values: 1.5 mM R *vs* 1.5 mM R + RPC, 1 month, $P = 0.008$; 3 months, $P = 0.004$. 2.5 mM R *vs* 2.5 mM R + RPC, 1 month, $P = 0.0004$; 3 months, $P = 0.00008$. (**d**–**i**) NeuN-stained retinas, 3 months post injection. Size bar = 200 μm. **d**, HBSS (saline) injected; **e**, DMSO; **f**, 1.5 mM R; **g**, 2.5 mM R; **h**, 1.5 mM R + pRPCs; **i**, 2.5 mM R + pRPCs, showing section containing pRPCs.

PCR

Retinal RNA extraction, semi-quantitative and qPCR were carried out and analysed as previously described.[14] QPCRs were carried out on 3–4 biological samples per category, each amplified in triplicate, giving 9–12 repeats in total.

Statistical analysis

Results were graphed in MS Excel. Error bars were calculated using standard error of the mean. The number of repetitions for each category is indicated within the figures themselves. *P*-values were calculated using the Student's *t*-test.

RESULTS

Stem cell transplantation

Native retinal cells of early postnatal origin can integrate and function as photoreceptors after subretinal transplantation.[12–14,18,19] We investigated whether newly-specified RGCs could be used intravitreally to treat optic neuropathies, using a rotenone-induced model of LHON. Retinas were dissociated from embryonic day 16 and 17 (E16 and E17) and postnatal Day2 (pn2) eGFP mice; within the timeframe for RGC specification.[20] 200 000 E16, E17 and pn2 freshly-harvested retinal cells were transplanted into 1.5 mM rotenone-treated eyes. After 1 month, eGFP + ve cell aggregations were present in the vitreous; but no evidence of retinal integration was found (data not shown). We therefore conclude that freshly dissociated, newly-specified RGCs did not provide beneficial effects to treat optic neuropathies in an analogous manner to the transplantation of newly-specified rod photoreceptors.

Previously, when cultured RPCs were subretinally injected as part of another study, we had noted transplanted cell adherence to the GCL, in instances where there had been leakage of cultured RPCs into the vitreous. Therefore, we then examined whether transplantation of cultured RPCs would achieve any therapeutic effect in rotenone-treated retinas. Cultured RPCs lose the ability to form photoreceptors and, when differentiated, form a mixture of glial cells with some neurons.[14,21] These cells are now thought to generate a neural/glial stem cell line with oligodendroglial potential, similar to neural stem cells isolated from the brain.[21] We injected 200 000 postnatally-derived early passage RPCs into 1.5 mM rotenone-treated retinas, transplanting both proliferating RPCs, and those that had undergone initial differentiation by withdrawal of Fgf2 from the medium for 5 days.

Both stages were tested, and in previous subretinal injections, cell adherence to the GCL had been noted for both. A small proportion of RPCs integrated along the inner-limiting membrane and GCL in the case of both proliferating RPCs (pRPCs, 0.131%) and differentiating cells (dRPCs 0.011%) (Figure 1a and b, Figure 1c–i = NeuN RGC counts). Notably, more pRPCs were retained than dRPCs after 1 month; pRPCs were therefore used in most subsequent studies. Cell counts were later obtained for 1.5 mM rotenone + pRPCs at 3 months and 2.5 mM rotenone + pRPCs at 1 and 3 months. Numbers of eGFP + ve RPCs retained after 3 months were dramatically reduced in comparison with the 1-month time-frame (Figure 1b).

MEMRI

Mice were treated with DMSO, 1.5 mM rotenone and 2.5 mM rotenone, followed 1 week later with an injection of 200 000 RPCs into the right eye. Transplants of both pRPCs and dRPCs were undertaken. The left eye was untreated. Animals were assessed by MEMRI 1 month after RPC transplantation (Figure 2a–h). Differences of signal intensity (S.I.) between rotenone-treated and rotenone + pRPC-treated animals were very significant ($P = 0.007$); differences between rotenone and rotenone + dRPC-treated animals just reached significance ($P = 0.046$; Figure 2g). To test whether the tissue of origin of the transplanted cells was of significance, we assessed MEF-treated animals using MEMRI (Figure 2g). S.I. differences between rotenone alone and rotenone and MEF-treated mice were not significant ($P = 0.091$). The effects of using a higher, more damaging dose of rotenone were also assessed, to compare results from RPC therapy with AAV-NDI1.[3] We added a 3-month time point at the higher dose of rotenone to evaluate the effects of cell therapy over time. Both 1 and 3 months post treatment, comparison of 2.5 mM rotenone alone *vs* 2.5 mM rotenone + pRPC-treated retinas gave significant results (1 month $P = 0.002$, 3 months $P = 0.02$) (Figure 2g and h).

Optokinetics

To test the functional benefits of RPC treatment on vision, we subjected wild type, DMSO-treated, 1.5 and 2.5 mM rotenone and 1.5 and 2.5 mM rotenone plus RPC-treated animals to optokinetic analysis. Improvements in vision were just statistically significant at the higher dose of rotenone at 1 month post treatment (1.5 mM rotenone *vs* 1.5 mM rotenone + RPCs, $P = 0.096$; 2.5 mM rotenone *vs* 2.5 mM rotenone + RPCs, $P = 0.046$), but, again, results obtained at 3 months were very significant (1.5 mM rotenone *vs* 1.5 mM rotenone + RPCs, $P = 0.005$; 2.5 mM rotenone *vs* 2.5 mM rotenone + RPCs, $P = 0.001$). Therefore, treatment of rotenone-damaged retinas with RPCs provided a beneficial effect (Figure 2i).

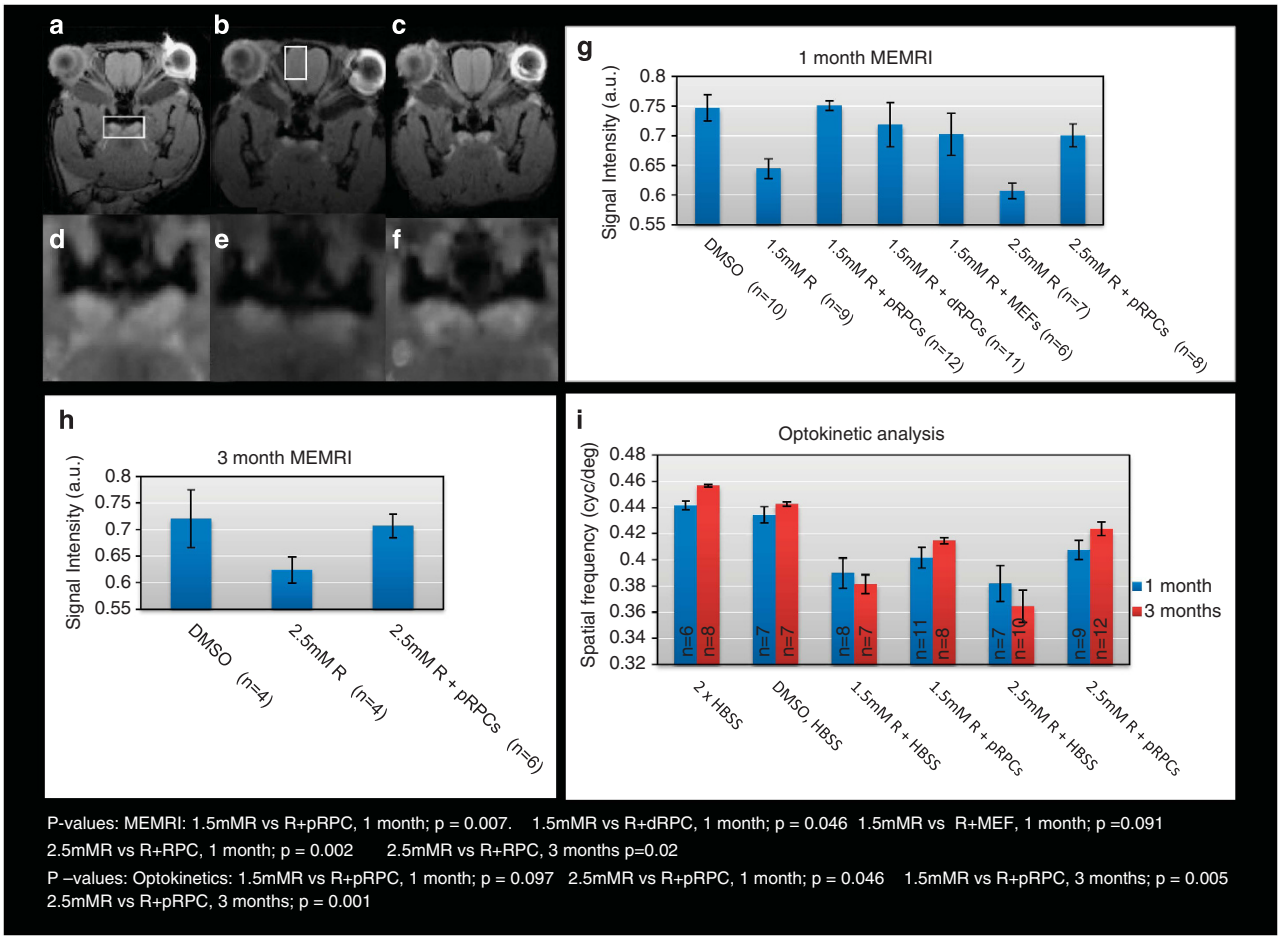

Figure 2 MEMRI and optokinetic analysis. **a** + **d**, DMSO; **b** + **e**, 2.5 mM Rotenone; **c** + **f**, 2.5 mM Rotenone + pRPCs. The box in A and enlarged images **d**–**f** indicate the region of interest (ROI) from within which the reference measurements were taken. The box in **b** indicates the area from which normalization measurements were taken. **g** + **h** show graphed 1 month and 3-month MEMRI intensity measurements. R, Rotenone; pRPC, proliferating RPC; dRPC, differentiating RPC; MEF, mouse embryonic fibroblasts. **i**, Optokinetic analysis at 1 and 3 months.

RGC counts

We used histology and NeuN staining to assess the effect of rotenone and cell treatment of rotenone-damaged retinas on the number of RGCs (Figure 1c–i). Cell counts were obtained from wild type, DMSO, 1.5 mM rotenone, 2.5 mM rotenone, 1.5 mM rotenone + pRPCs and 2.5 mM rotenone + pRPC-treated eyes at both 1 month and 3-month time points. Differences between 1.5 mM rotenone and 1.5 mM rotenone + RPC-treated samples were significant at both stages (1 month, $P = 0.008$; 3months, $P = 0.004$). Comparisons between 2.5 mM rotenone-treated samples and 2.5 mM rotenone + RPC-treated samples were highly significant (1 month, $P = 0.0004$; 3 months, $P = 0.00008$). GCL numbers were significantly higher in all rotenone and rotenone-RPC-treated animals at 3 months; comparison of 1 month with 3 months 1.5 mM rotenone-treated eyes provided significant evidence of greater RGC numbers at 3 months; $P = 0.002$ (Figure 1c). Conversely, numbers of transplanted eGFP + ve cells were much lower at 3 months. Furthermore, eGFP-positive cells rarely stained with NeuN, nor did rotenone + RPC-treated eyes achieve cell counts equivalent to DMSO controls. The therapeutic effect was therefore not owing to the integration of transplanted RGCs. Rotenone caused a dip in staining intensity of NeuN-positive cells, in addition to cell number reductions (Figure 1f and g). We suspect that some severely damaged RGCs showed negligible staining at 1 month but demonstrated partial recovery by 3 months, as evaluated by greater numbers of NeuN-expressing cells.

Molecular markers

The mechanism of action underlying the therapeutic effects provided by intravitreal injection of pRPCs is unclear and would best be tackled via genomic-scale analysis (which is beyond the scope of this study). We did, however, investigate the expression of a number of candidate genes. An initial screening process was carried out using semi-quantitative PCR on samples from DMSO, rotenone, and rotenone + RPC-treated animals at 1 month (as a significant amount of recovery seemed to have taken place by 3 months (Figure 1c)). Genes that were chosen on the basis of mitochondrial function (MTND1, 4, 6, Cox4i2, Cox6a2, NdufaF1), were glial markers (GFAP), GCL markers (Sncg, CHaT, Atoh7, Gad1, Gabbr, Isl1, Rbfox3, Syp, Th, Thy1), those that had apoptotic/cell cycle functions (Ccd1, Ki67, Bad, Bax, Bcl2) or were rotenone responsive and upregulated in glaucoma (Hba-a1, Hbb-b1 and 2).[22,23]

Following the initial screening process, we included RPC-treated samples and rescreened rotenone responsive genes via qPCR. Nine genes showed differential expression in response to the treatment; MTND1 is also shown as it is mutated in LHON (see Figure 3a–j). *P*-values are shown; significant changes are shaded in green (Figure 3k). Bax and Bcl2, pro- and antiapoptotic genes, are expressed at low levels in DMSO controls, raised in rotenone-treated samples and are higher again in rotenone + RPC-treated samples. Bcl2, which is antiapoptotic, shows a much greater increase in response to treatment. Changes are also seen with Cox4i1, a nuclear-encoded subunit of cytochrome *c* oxidase, the terminal enzyme in the mitochondrial electron transport chain, NdufaF1, a complex 1 assembly factor, and MTND4 and MTND6, mitochondrial complex1 subunits mutated in LHON. GFAP expression rose dramatically in response to treatment with RPCs, suggesting higher glial activity (confirmed by immunohistochemistry, see Figure 4). Hba-a1 was downregulated after rotenone treatment as expected[22] and upregulated in RPC-treated samples. Hba-a1 is expressed in the apoptosis-like processes that take place as differentiating lens fibre cells lose their nuclei, without dying.[24] It is also present in the retina, optic nerve head macroglia and RGCs, and is upregulated in glaucomatous eyes and is prominently expressed in retinal glia.[23] Upregulation could relate to antiapoptotic function, or be protective against damage-induced hypoxia.[23,24]

DISCUSSION

Treatment of rotenone-damaged retinas with RPCs generates a notable therapeutic effect. The mode of action of RPC therapy in this LHON model is unknown, however, there are a number of possibilities. Growth factors secreted by the transplanted cells may be augmenting natural physiological processes leading to RGC recovery, immunological reaction to the transplanted cells may be enhancing natural repair processes, or glial functions carried out by transplanted pRPC cells may be protective to RGCs.

The transplanted pRPCs tend to line up along the GCL, but do not integrate within the GCL as RGCs; NeuN staining does not demonstrate the appearance of eGFP-positive RGCs, however, transplanted RPCs do stain with GFAP, the levels of which are generally raised in retinas which have received RPCs (Figure 3e and k, Figure 4). Levels of Hba-a1 are raised in rotenone + RPC-treated samples; Hb in retinal glial cells has been previously described as 'prominently detectable'.[23] These data point to increased glial function after pRPC transplantation. RPC transplants may not be as well protected immunologically as photoreceptor transplants; a few hundred GCL-associated cells remain after 1 month and are reduced again by 3 months. Subretinal photoreceptor transplants of similar cell numbers initially showed retention of 1000 cells after 1 month,[12,13,18] with reductions after 4 months owing to a chronic immunological response.[25] Despite reductions in transplanted cells, repair of damaged retinas is more significant after 3 months than after one, as judged by both RGC counts and by optokinetics. Therefore, it is likely that the effects of cell transplantation are independent of the ongoing presence of transplanted RPCs and may relate to processes that occur in the first few days or weeks post transplantation.

The mechanism of action of stem cell therapies has long been a matter for debate. Initial theories were based on differentiation of stem cells in the site of transplantation and replacement of damaged tissue. This can be shown to be the case with photoreceptor transplants,[13] but may not be the case for other stem cells delivered to other sites in the body, with a paracrine mode of action favoured for some.[26–28] In this case, the premise is that secretion of hormones, growth factors and/or extracellular matrix components by the stem cells, in complex dialogue with pre-existing damaged tissue, may be stimulating transplanted cells to secrete therapeutic substances in response to the injured host tissue, thereby providing benefit.[26–28] The addition of pRPCs with glial potential to damaged retinas may enhance natural repair processes, by physical contact and structural repair, by providing an antiapoptotic effect (as suggested by increased Bcl2 levels), and by secretion of hormones and/or growth factors[26–28] or, perhaps, via increased glial protection of normally unmyelinated segments of ganglion cell axons.[21] RGC axons, anterior to the lamina cribrosa, are unmyelinated, resulting in much less energy-efficient generation and propagation of action potentials. This axonal region contains more mitochondria in part to compensate for the lack of myelination,[4] an anatomical feature that probably underlies RGC vulnerability to traumas such as mitochondrial dysfunction, increased intraocular pressure (glaucoma) and demyelination beyond the lamina cribrosa in optic neuritis (multiple sclerosis and other demyelinating disorders). However, intraretinal portions of RGC axons are myelinated abnormally in 1% of the human population.[21,29,30] Abnormal myelination leads to a decrease in

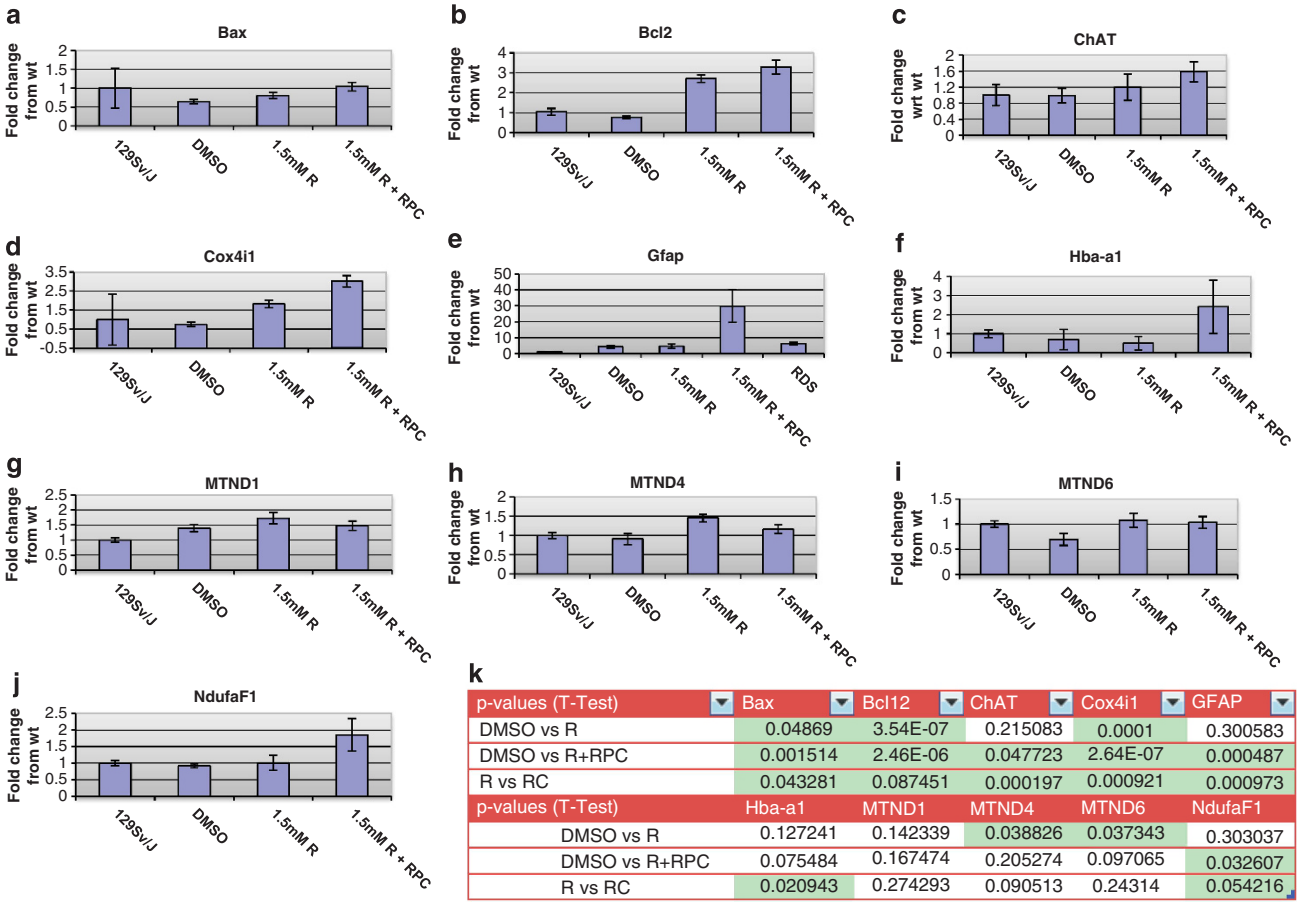

k

p-values (T-Test)	Bax	Bcl12	ChAT	Cox4i1	GFAP
DMSO vs R	0.04869	3.54E-07	0.215083	0.0001	0.300583
DMSO vs R+RPC	0.001514	2.46E-06	0.047723	2.64E-07	0.000487
R vs RC	0.043281	0.087451	0.000197	0.000921	0.000973
p-values (T-Test)	Hba-a1	MTND1	MTND4	MTND6	NdufaF1
DMSO vs R	0.127241	0.142339	0.038826	0.037343	0.303037
DMSO vs R+RPC	0.075484	0.167474	0.205274	0.097065	0.032607
R vs RC	0.020943	0.274293	0.090513	0.24314	0.054216

Figure 3 Molecular Markers. (**a**–**j**): qPCR of genes with expression changes in response to rotenone damage; and to treatment. **a**, Bax; **b**, Bcl2; **c**, ChAT; **d**, Cox4i1 **e**, GFAP; **f**, Hba-a1; **g**, MTND1; **h**, MTND4; **i**, MTND6; **j**, NdufaF1; **k**, *P*-value table; significant results are highlighted in green ($P<0.05$).

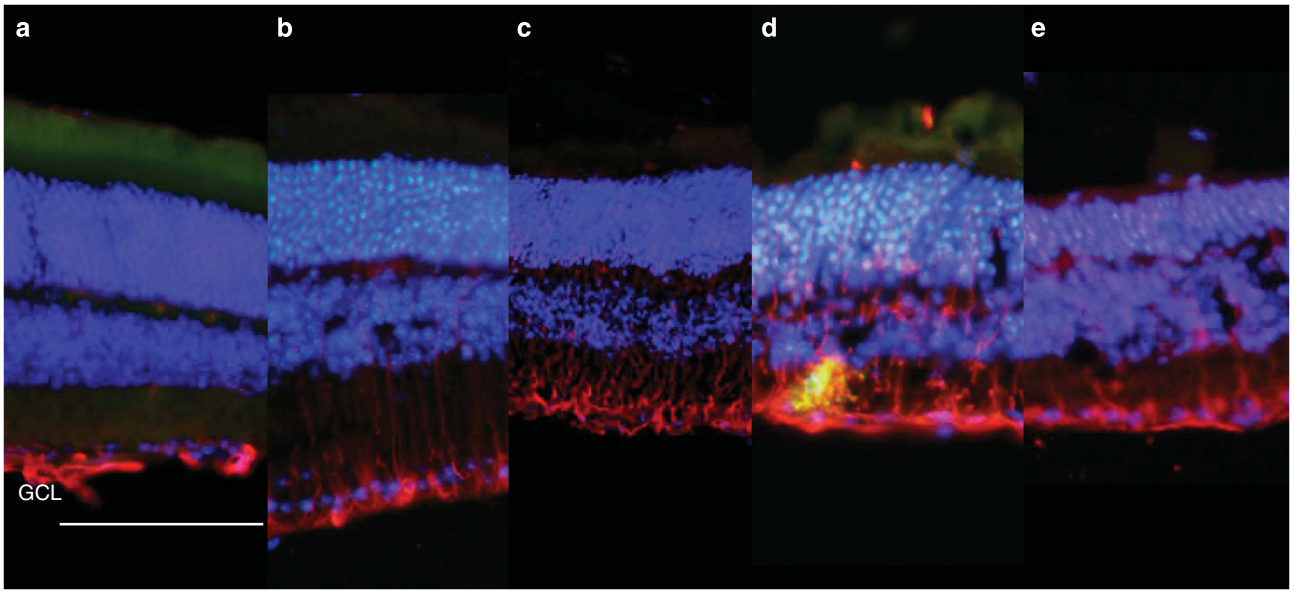

Figure 4 GFAP staining of controls and treated eyes. **a**, untreated 129Sv/J; **b**, DMSO; **c**, 1.5 mM rotenone (1 month); **d**, 1.5 mM Rotenone + pRPCs (1 month); **e**, RDS RP retina, untreated. Size bar = 100 μm.

visual acuity, an increased incidence of degeneration in myelinated nerves, and visual field defects.[29,30] Myelinating oligodendrocytes are normally absent from the retina, but can be generated *in vitro* from RPCs.[21] It should be noted, however, that myelinating oligodendrocytes were generated from RPCs after growth in medium containing Fgf2, PDGF and forskolin,[21] a protocol not followed in the

current study. Furthermore, RPC treatment in this case seemed to have beneficial, not detrimental, effects on vision.

A broad range of gene- and cell-based therapies are being contemplated for retinal degenerations.[2,13,16,18,31] Specifically, preclinical studies have provided evidence that a number of gene therapies may provide beneficial effects for LHON.[2,3,32,33] Of note, results obtained from this study provide the first demonstration that therapeutic effects may be obtained using a stem cell-based approach for LHON. A number of RPC-secreted factors may be aiding recovery from rotenone-induced trauma and may be of assistance in treating a wide range of optic nerve pathologies. Identification of such factors may permit their therapeutic testing independently of cell transplantation, which would permit the avoidance of cell sourcing, ethical, safety and immunological issues associated with cell transplantation.

CONFLICT OF INTEREST

Professor Farrar and Dr Kenna are directors of Genable Technologies; Dr Chadderton is a consultant for Genable Technologies, Dr Mansergh and Dr Gobbo declare no conflict of interest.

ACKNOWLEDGEMENTS

We would like to thank the staff of the Bioresources Unit, Trinity College Dublin, for technical assistance, Rustam Rakhmatullin for technical assistance with MEMRI and Dr Michael Wride for helpful discussion and critical reading of this manuscript. We would also like to thank Don Zack for his gift of the eGFP transgenic mice. This research was funded by Fighting Blindness Ireland, the Health Research Board of Ireland (HRB) and Science Foundation Ireland (SFI).

1 Yu-Wai-Man P, Griffiths PG, Hudson G *et al*: Inherited mitochondrial optic neuropathies. *J Med Genet* 2009; **46**: 145–158.
2 Farrar GJ, Chadderton N, Kenna PF *et al*: Mitochondrial disorders: aetiologies, models systems, and candidate therapies. *Trends Genet* 2013; **29**: 488–497.
3 Chadderton N, Palfi A, Millington-Ward S *et al*: J. Intravitreal delivery of AAV-NDI1 provides functional benefit in a murine model of Leber hereditary optic neuropathy. *Eur J Hum Genet* 2013; **21**: 62–68.
4 Yu-Wai-Man P, Griffiths PG, Chinnery PF: Mitochondrial optic neuropathies- disease mechanisms and therapeutic strategies. *Prog Retin Eye Res* 2011; **30**: 81–114.
5 Lin CS, Sharpley MS, Fan W: Mouse mtDNA mutant model of Leber hereditary optic neuropathy. *Proc Natl Acad Sci USA* 2012; **109**: 20065–20070.
6 Alexander C, Votruba M, Pesch UE *et al*: OPA1, encoding a dynamin-related GTPase, is mutated in autosomal dominant optic atrophy linked to chromosome 3q28. *Nat Genet* 2000; **26**: 211–215.
7 Aung T, Ocaka L, Ebenezer ND *et al*: A major marker for normal tension glaucoma: association with polymorphisms in the OPA1 gene. *Hum Genet* 2002; **110**: 52–56.
8 Lee S, Sheck L, Crowston JG *et al*: Impaired complex-I-linked respiration and ATP synthesis in primary open-angle glaucoma patient lymphoblasts. *Invest Ophthalmol Vis Sci* 2012; **53**: 2431–2437.
9 Zhang X, Jones D, Gonzalez-Lima F: Mouse model of optic neuropathy caused by mitochondrial complex I dysfunction. *Neurosci Lett* 2002; **326**: 97–100.
10 Zhang X, Jones D, Gonzalez-Lima F: Neurodegeneration produced by rotenone in the mouse retina: a potential model to investigate environmental pesticide contributions to neurodegenerative diseases. *J Toxicol Environ Health A* 2006; **69**: 1681–1697.
11 Hayworth CR, Rojas JC, Gonzalez-Lima F: Transgenic mice expressing cyan fluorescent protein as a reporter strain to detect the effects of rotenone toxicity on retinal ganglion cells. *J Toxicol Environ Health A* 2008; **71**: 1582–1592.
12 Bartsch U, Oriyakhel W, Kenna PF *et al*: Retinal cells integrate into the outer nuclear layer and differentiate into mature photoreceptors after subretinal transplantation into adult mice. *Exp Eye Res* 2008; **86**: 691–700.
13 West E, Pearson R, Duran Y *et al*: Manipulation of the recipient retinal environment by ectopic expression of neurotrophic growth factors can improve transplanted photoreceptor integration and survival. *Cell Transplant* 2012; **21**: 871–887.
14 Mansergh FC, Vawda R, Millington-Ward S *et al*: Loss of photoreceptor potential from retinal progenitor cell cultures, despite improvements in survival. *Exp Eye Res* 2010; **91**: 500–512.
15 Mansergh F, Orton NC, Vessey JP *et al*: Mutation of the calcium channel gene Cacna1f disrupts calcium signaling, synaptic transmission and cellular organization in mouse retina. *Hum Mol Genet* 2005; **14**: 3035–3046.
16 Kiang S, Palfi A, Ader M *et al*: Toward a gene therapy for dominant disease; validation of an RNA interference based mutation independent approach. *Mol Ther* 2005; **12**: 555–561.
17 Pautler RG: Biological applications of manganese-enhanced magnetic resonance imaging. *Methods Mol Med* 2006; **124**: 365–386.
18 MacLaren RE, Pearson RA, MacNeil A *et al*: Retinal repair by transplantation of photoreceptor precursors. *Nature* 2006; **444**: 203–207.
19 Eberle D, Kurth T, Santos-Ferreira T *et al*: Outer segment formation of transplanted photoreceptor precursor cells. *PLoS One* 2012; **7**: e46305.
20 Wallace VA: Concise review: making a retina—from the building blocks to clinical applications. *Stem Cells* 2011; **29**: 412–417.
21 Czekaj M, Haas J, Gebhardt M *et al*: In vitro expanded stem cells from the developing retina fail to generate photoreceptors but differentiate into myelinating oligodendrocytes. *PLoS One* 2012; **7**: e41798.
22 Richter F, Meurers BH, Zhu C *et al*: Neurons express hemoglobin alpha- and beta-chains in rat and human brains. *J Comp Neurol* 2009; **515**: 538–547.
23 Tezel G, Yang X, Luo C *et al*: Hemoglobin expression and regulation in glaucoma: insights into retinal ganglion cell oxygenation. *Invest Ophthalmol Vis Sci* 2010; **51**: 907–919.
24 Mansergh FC, Hunter SM, Geatrell JC *et al*: Developmentally regulated expression of hemoglobin subunits in avascular tissues. *Int J Dev Biol* 2008; **52**: 873–886.
25 West EL, Pearson RA, Barker SE *et al*: Long-term survival of photoreceptors transplanted into the adult murine neural retina requires immune modulation. *Stem Cells* 2010; **28**: 1997–2007.
26 O'Brien T, Barry FP: Stem cell therapy and regenerative medicine. *Mayo Clin Proc* 2009; **84**: 859–861.
27 Ratajczak MZ, Kucia M, Jadczyk T *et al*: Pivotal role of paracrine effects in stem cell therapies in regenerative medicine: can we translate stem cell-secreted paracrine factors and microvesicles into better therapeutic strategies? *Leukemia* 2012; **26**: 1166–1173.
28 Manuguerra-Gagné R, Boulos PR, Ammar A *et al*: Transplantation of mesenchymal stem cells promotes tissue regeneration in a glaucoma model through laser-induced paracrine factor secretion and progenitor cell recruitment. *Stem Cells* 2013; **31**: 1136–1148.
29 FitzGibbon T, Nestorovski Z: Morphological consequences of myelination in the human retina. *Exp Eye Res* 1997; **65**: 809–819.
30 Duval R, Hammamji K, Aroichane M *et al*: Acquired myelinated nerve fibers in association with optic disk drusen. *J AAPOS* 2010; **14**: 544–547.
31 Stieger K, Cronin T, Bennett J, Rolling F: Adeno-associated virus mediated gene therapy for retinal degenerative diseases. *Methods Mol Biol* 2011; **807**: 179–218.
32 Ellouze S, Augustin S, Bouaita A *et al*: Optimized allotopic expression of the human mitochondrial ND4 prevents blindness in a rat model of mitochondrial dysfunction. *Am J Hum Genet* 2008; **83**: 373–387.
33 Yu H, Koilkonda RD, Chou TH *et al*: Gene delivery to mitochondria by targeting modified adeno-associated virus suppresses Leber's hereditary optic neuropathy in a mouse model. *Proc Natl Acad Sci USA* 2012; **109**: E1238–E1247.